A Mathematically Simple Turbulence Closure Model for Attached and Separated Turbulent Boundary Layers

D. A. Johnson* and L. S. King*
NASA Ames Research Center, Moffett Field, California

A new turbulence closure model designed specifically to treat two-dimensional, turbulent boundary layers with strong adverse pressure gradients and attendant separation is presented. The influence of history effects are modeled by using an ordinary differential equation derived from the turbulent kinetic energy equation to describe the streamwise development of the maximum Reynolds shear stress in conjunction with an assumed eddy viscosity distribution that has as its velocity scale the maximum Reynolds shear stress. In the outer part of the boundary layer, the eddy viscosity is treated as a free parameter which is adjusted in order to satisfy the ODE for the maximum shear stress. Because of this, the model is not simply an eddy viscosity model, but contains features of a Reynolds stress model. Comparisons with experiment are presented that clearly show the proposed model to be superior to the Cebeci-Smith one in treating strongly retarded and separated flows. In contrast to two-equation, eddy viscosity models, it requires only slightly more computational effort than simple models such as the Cebeci-Smith.

Nomenclature

a_1 = modeling constant, $-\overline{u'v'_m}/k_m$
A^+ = van Driest damping constant
c = chord length
C_{dif} = turbulent diffusion modeling constant
C_{fe} = local skin-friction coefficient based on edge conditions
C_p = pressure coefficient
D = near-wall damping term, $D=(1-\exp^{-y/A})$, $A=A^+f[u_\tau,\nu,(\mathrm{d}p/\mathrm{d}x)]$
$\mathfrak{D}$ = turbulent diffusion rate
g = variable change
H = boundary-layer shape factor
k = turbulence kinetic energy
L = dissipation length scale
p = pressure
q^2 = turbulent flow property, $u'^2+v'^2+w'^2$
u = streamwise velocity component
u_τ = wall shear velocity
v = normal velocity component
v = turbulent diffusion convection velocity
x = coordinate in streamwise direction
y = coordinate in normal direction
α = angle of attack
γ = Klebanoff's intermittency function
δ = boundary-layer thickness
δ^* = boundary-layer displacement thickness
δ_i^* = incompressible boundary-layer displacement thickness
ϵ = dissipation rate
κ = von Kármán's constant
ν = kinematic viscosity
ν_t = turbulent eddy viscosity
ρ = density
τ_t = turbulent Reynolds shear stress

Subscripts

e = boundary-layer edge conditions
eq = equilibrium conditions
i = inner part of boundary layer
m = values of quantity where $-\overline{u'v'}$ is a maximum
o = outer part of boundary layer
∞ = freestream conditions

Superscripts

$(\ )'$ = fluctuating quantity
$(\bar{\ })$ = time-averaged quantity

Introduction

ACCURATE theoretical predictions of airfoil performance up to and beyond stall require that the turbulent boundary layer and wake be correctly described. For finite difference, viscous flow calculation methods, the accuracy to which this can be done depends on the validity of the closure model used to describe the turbulent Reynolds stresses. Thus, the turbulence closure model is fundamental to these methods. Bradshaw[1] put this in another way: "A numerical procedure without a turbulence closure model stands in the same relation to a complete calculation method as an ox does to a bull."

In this paper, a new turbulence closure model formulation is presented. Based on comparisons with experiment, this new model appears capable of treating two-dimensional, subsonic, pressure-driven separated flows and transonic, shock-induced separated flows. New modeling assumptions are applied that evolved from 1) recent measurements of turbulent flow properties in separated boundary layers (made possible with the development of the laser velocimeter technique) and 2) insights gained from the comparison of these experimental results with theoretical predictions based on existing turbulence closure models.

A new approach is taken to model the strong "history" effects characteristic of turbulent boundary layers subjected to rapid changes in the streamwise pressure gradient. An ordinary differential equation (ODE), derived from the turbulence kinetic energy equation, is used to describe the streamwise development of the maximum Reynolds shear stress in conjunction with an assumed eddy viscosity distribution that has as its velocity scale the maximum Reynolds shear stress. In the outer part of the boundary layer, the eddy viscosity is treated as a free parameter that is adjusted to satisfy the ODE for the maximum Reynolds shear stress. Because of this, the model is not simply an eddy

Presented as Paper 84-0175 at the AIAA 22nd Aerospace Sciences Meeting, Reno, NV, Jan. 9-12, 1984; received Feb. 29, 1984; revision received Feb. 7, 1985. This paper is declared a work of the U.S. Government and therefore is in the public domain.

*Research Scientist. Member AIAA.

viscosity model, but also contains features of a Reynolds stress model. Since only an ODE needs to be solved with this model rather than one or more partial differential equations, the proposed closure model requires only slightly more computational effort than algebraic models such as the Cebeci-Smith.[2]

The performance of this closure model will be illustrated through comparisons with experiment for three difficult flow cases: 1) a transonic shock-induced separated flow,[3] 2) a low-speed diffuser flow with separation,[4] and 3) a supercritical airfoil at transonic conditions.[5] The first two flow cases contain large regions of separated flow; the third contains only a small separated zone near the trailing edge of the airfoil. Included in these comparisons are results obtained with the popular Cebeci-Smith model.

Discussion

Closure Model Formulation

In recent years, considerable effort has been directed toward incorporating two-equation (e.g., $k-\epsilon$ and $k-\omega^2$), eddy viscosity formulations into numerical prediction methods with the expectation of improved predictive accuracy for strong inviscid-viscous interaction cases. Weighed against the added numerical complexity and computational time required to solve two additional partial differential equations, the improvements in predictive accuracy over algebraic models, such as the Cebeci-Smith, have not been dramatic. In general, the two-equation formulations do better than the algebraic formulations for separated flow cases, in that the rapid skin-friction recovery observed experimentally downstream of reattachment is better predicted and the calculated mean velocity profiles within the separated zone are in better qualitative agreement with experiment. Yet for transonic cases with massive separation, the prediction of surface pressure has been less than satisfactory (e.g., Ref. 6). For cases in which the flow remains attached, results have even been obtained that could be construed as inferior to those obtained with the Cebeci-Smith model (e.g., Ref. 7).

The development of the present closure model was based on a completely different philosophy from that used in developing the two-equation formulations. The goal was to develop an adequate closure model for a limited class of flows rather than a universal model. The following premise motivated the development. If the Cebeci-Smith model can perform as well as it does with the known invalid assumption that the turbulent shear stress depends only on local properties of the mean flow, then it should be possible to develop a better closure model for boundary-layer flows without attempting to predict, throughout the entire viscous layer, the production, dissipation, and diffusion of both the turbulence kinetic energy and the dissipation rate, as is done in two-equation formulations. For rapidly varying flows, it is postulated that a proper accounting of convection effects was essential, with diffusion effects playing a less dominant role.

To account for convection and diffusion effects on the Reynolds shear stress development, an ODE is proposed to prescribe the maximum Reynolds shear stress development in the streamwise direction. More precisely, the ODE describes the development of $-\overline{u'v'_m}$ along the path of maximum shear stress and is derived from the turbulence kinetic energy equation. For convenience, in this paper $-\overline{u'v'}$ will be referred to as the Reynolds shear stress τ_t, although it is really given by $\tau_t/\bar{\rho}$. Along with this ODE for the maximum Reynolds shear stress $-\overline{u'v'_m}$, an eddy viscosity distribution is assumed across the boundary layer that is functionally dependent on $-\overline{u'v'_m}$. This eddy viscosity distribution will be described first.

The following functional form for the eddy viscosity ν_t is assumed:

$$\nu_t = \nu_{to}[1-\exp(-\nu_{ti}/\nu_{to})] \tag{1}$$

where ν_{ti} and ν_{to} can be thought of as describing the eddy viscosity in the inner and outer parts of the boundary layer. Notice in Eq. (1) that $\nu_t \approx \nu_{ti}$ when $\nu_{ti} \ll \nu_{to}$ and that $\nu_t \approx \nu_{to}$ when $\nu_{ti} \gg \nu_{to}$. Thus, Eq. (1) provides a smooth blending between the regions where $\nu_t \approx \nu_{ti}$ and where $\nu_t \approx \nu_{to}$. It also makes ν_t functionally dependent on ν_{to} across most of the boundary layer. This is a critical element of the proposed closure model since ν_{to}, as will be described shortly, is used to control the rate of growth of $-\overline{u'v'_m}$. The inner eddy viscosity ν_{ti} is assumed to be given by the following relationship:

$$\nu_{ti} = D^2\kappa y(-\overline{u'v'_m})^{1/2} \tag{2}$$

where D is the same damping term used in the Cebeci-Smith formulation. Typically, in zero-equation, eddy viscosity models, the eddy viscosity in the inner part of the boundary layer is represented by $D^2\kappa^2y^2|\partial\bar{u}/\partial y|$. For zero-pressure-gradient boundary layers, Eq. (2) reduces to that form; however, for nonzero-pressure-gradient flows, it is believed that Eq. (2) is more broadly valid. This will be illustrated when the results obtained with the proposed closure model are compared with those obtained with the Cebeci-Smith model. An adjustment in the damping term D is required in Eq. (2) to account for a y dependency instead of a y^2 dependency in the near-wall region. This is done by simply using a value of 15 for A^+ rather than the usual value of 26 used in the Cebeci-Smith model.

The outer eddy viscosity ν_{to} is assumed to have the distribution

$$\nu_{to} = \text{const}\cdot\gamma \tag{3}$$

where γ is Klebanoff's intermittency function, $\gamma = 1/[1+5.5(y/\delta)^6]$. The constant in Eq. (3) is determined by the value of $-\overline{u'v'_m}$ prescribed by the ODE mentioned earlier. That is, the constant is adjusted as needed such that the following relationship is satisfied:

$$\nu_t|_m = \frac{-\overline{u'v'_m}}{(\partial\bar{u}/\partial y)|_m} = \underbrace{\frac{(-\overline{u'v'_m})^{1/2}}{(\partial\bar{u}/\partial y)|_m}}_{\text{length scale}} \underbrace{(-\overline{u'v'_m})^{1/2}}_{\text{velocity scale}} \tag{4}$$

where ν_t is given by Eq. (1). The subscript m denotes that the quantity is evaluated where $-\overline{u'v'}$ is a maximum. The strain rate in Eq. (4), $(\partial\bar{u}/\partial y)|_m$, like δ and δ^*, is a determinable property of the mean velocity profile. For convience, the boundary-layer approximation for the strain rate has been used. To indicate that the eddy viscosity at the location of $-\overline{u'v'_m}$ can be represented as the product of a length scale and a velocity scale, the right-hand side of Eq. (4) is shown in two forms. The length scale is given by $(-\overline{u'v'_m})^{1/2}/(\partial\bar{u}/\partial y)|_m$ and the velocity scale by $(-\overline{u'v'_m})^{1/2}$. For the inner eddy viscosity representation [see Eq. (2)], the velocity scale is also $(-\overline{u'v'_m})^{1/2}$, but the length scale is κy. The use of $(-\overline{u'v'_m})^{1/2}$ as the velocity scale is supported by the work of Perry and Schofield.[8] For boundary-layer flows with adverse pressure gradients they found that this quantity provided a much better velocity defect correlation than did the wall shear velocity u_τ.

The adjustment of ν_{to} in order to satisfy the ODE for $-\overline{u'v'_m}$ and the use of $(-\overline{u'v'_m})^{1/2}$ as the velocity scale for the eddy viscosity, make this closure model strongly dependent on the Reynolds shear stress devleopment. Because of this, the authors consider the closure model to be a hybrid Reynolds stress/eddy viscosity model rather than simply an eddy viscosity model. The eddy viscosity hypothesis is used to determine the shear stress distribution across the boundary layer, but it is the Reynolds shear stress ODE that determines the level of the shear stress.

To complete the formulation, an equation is needed for $-\overline{u'v'_m}$. This equation is developed from the turbulence kinetic energy equation, using similar assumptions to those used by Bradshaw et al.[9] in the development of their approximate Reynolds stress model. Along the path s of maximum kinetic energy κ, the turbulence kinetic energy equation for an incompressible boundary layer reduces to

$$\bar{u}_m \frac{dk_m}{dx} = -\overline{u'v'_m}\frac{\partial \bar{u}}{\partial y}\bigg|_m - \frac{\partial}{\partial y}\left(\frac{\overline{p'v'}}{\rho} + \frac{1}{2}\overline{q^2 v'}\right)\bigg|_m - \epsilon_m \tag{5}$$

convection | production | diffusion | dissipation

The approximations have been made that x and s are nearly coincident and that y is nearly normal to s. The m denotes that the quantity is evaluated where k or $-\overline{u'v'}$ is a maximum. This equation is also valid for compressible (subsonic and transonic) boundary layers, if mass-averaged variables are employed.[10]

To simplify this equation further, a dissipation length scale L_m is defined as

$$L_m = (-\overline{u'v'_m})^{3/2}/\epsilon_m$$

and the assumption $(-\overline{u'v'_m}/k_m) = a_1 = \text{const}$ is introduced. Upon rearrangement, Eq. (5) takes the form

$$(-\overline{u'v'_m})^{1/2} = L_m \frac{\partial \bar{u}}{\partial y}\bigg|_m - \frac{L_m}{(-\overline{u'v'_m})}\mathfrak{D}_m - \frac{L_m \bar{u}_m}{a_1(-\overline{u'v'_m})}\frac{d(-\overline{u'v'_m})}{dx} \tag{6}$$

contribution due to diffusion | contribution due to convection

For convenience, the turbulent diffusion term is represented in Eq. (6) by $\mathfrak{D}_m$.

This ordinary differential equation has been employed in the development of integral boundary-layer methods by McDonald[11] and Green et al.[12] In the former method, it is used to obtain an expression for the shear stress integral (the integrated value of the Reynolds shear stress across the boundary layer), whereas in the latter method it is used to obtain an expression for the entrainment coefficient.

The dissipation length scale L_m is assumed to scale with y in the inner part of the boundary layer and with the boundary-layer thickness δ in the outer part of the boundary layer. The functional form assumed for L_m is

$$L_m = 0.4y_m \quad y_m/\delta \le 0.225$$

$$L_m = 0.09\delta \quad y_m/\delta > 0.225 \tag{7}$$

In Eq. (6), $L_m(\partial\bar{u}/\partial y)|_m$ can be interpreted as the square root of the turbulent shear stress that would result if convection and diffusion effects were negligibly small. This term is thus replaced by the quantity $(-\overline{u'v'_{m,\,eq}})^{1/2}$, which is assumed to be determined from the following equilibrium eddy viscosity distribution:

$$\nu_{t,\,eq} = \nu_{to,\,eq}[1 - \exp(\nu_{ti,\,eq}/\nu_{to,\,eq})] \tag{8a}$$

$$\nu_{ti,\,eq} = D^2 \kappa y (-\overline{u'v'_{m,\,eq}})^{1/2} \tag{8b}$$

$$\nu_{to,\,eq} = 0.0168 u_e \delta_i^* \gamma \tag{8c}$$

The only remaining unknown quantity is $\mathfrak{D}_m$, the turbulent diffusion along the path of maximum $-\overline{u'v'}$. This quantity is approximated by the following expression:

$$\mathfrak{D}_m = \frac{C_{dif}(-\overline{u'v'_m})^{3/2}}{a_1\delta[0.7 - (y/\delta)_m]}\left|1 - \left(\frac{\nu_{to}}{\nu_{to,\,eq}}\right)^{1/2}\right| \tag{9}$$

where C_{dif} is a modeling constant. The formulation of this expression is given in the Appendix.

To solve Eq. (6), it is advantageous to make the following change of variables:

$$g = (-\overline{u'v'_m})^{-1/2} \text{ and } g_{eq} = (-\overline{u'v'_{m,\,eq}})^{-1/2} \tag{10}$$

Introducing this change in variables and the modeled equation for $\mathfrak{D}_m$ results in Eq. (6) taking the form used in the implementation of this closure model,

$$\frac{dg}{dx} = \frac{a_1}{2\bar{u}_m L_m}\left[\left(1 - \frac{g}{g_{eq}}\right) + \frac{C_{dif}L_m}{a_1\delta[0.7 - (y/\delta)_m]}\left|1 - \left(\frac{\nu_{to}}{\nu_{to,\,eq}}\right)^{1/2}\right|\right] \tag{11}$$

convective change | imbalance between production and dissipation | contribution due to diffusion

This equation is locally linearized by approximating all the quantities except g *and* g_{eq} by their values at the previous x station. This approximation is also applied to $-\overline{u'v'_m}$ and $-\overline{u'v'_{m,\,eq}}$ in Eqs. (2) and (8b), respectively.

The closure model that has been developed can be summarized as being composed of three parts: 1) a nonequilibrium eddy viscosity distribution [Eqs. (1-4)], 2) a rate equation [Eq. (11)] for the streamwise development of $-\overline{u'v'_m}$, and 3) an equilibrium (production = dissipation) eddy viscosity distribution [Eqs. (8)]. The equilibrium eddy viscosity model of Eq. (8) plays several important roles. First, it is used to determine g_{eq} and $\nu_{to,\,eq}$ in Eq. (11). It also is the resultant eddy viscosity distribution when $dg/dx \approx 0$. Finally, it is used as the initial eddy viscosity distribution in starting the calculations.

With the proposed closure model, initial conditions for Eq. (11) are needed in addition to a mean streamwise velocity profile and a value for $-\overline{u'v'_m}$ to start a calculation. The most straightforward approach is to assume that the flow is in equilibrium at the start of the calculations,

$$\nu_t = \nu_{t,\,eq} \text{ and } g = g_{eq}\left(\text{i.e., } \frac{dg}{dx} = 0\right) \tag{12}$$

In this case, a value of $-\overline{u'v'_{m,\,eq}}$ is needed. This quantity can be an experimental value or a value determined from an equilibrium eddy viscosity model such as the Cebeci-Smith. Alternatively, the wall shear velocity u_τ, as determined either from experiment or from calculations, can be used. The starting mean velcoity profile can either be a calculated or an experimental profile. Obviously, the calculations should not be started where the shear stress is changing rapidly in the streamwise direction, such as near the point where turbulent transition is initiated.

In the next section, the performance of this closure model is illustrated through comparison with experiment. All of the calculations to be presented were obtained for a value of 0.25 and 0.50 for a_1 and C_{dif}, respectively. Experimentally, a_1 is observed to vary between 0.2 and 0.3. The turbulent diffusion in boundary-layer flows is less well established. However, the calculations were found to be relatively insensitive to the modeled form of the diffusion term.

Closure Model Performance

The closure model just described has been incorporated into the finite difference (direct/inverse) boundary-layer program of Carter.[13] The boundary-layer equations are not truly predictive, since either the pressure gradient (direct mode) or a mass flux parameter $\rho_e u_e \delta^*$ (inverse mode) must be prescribed as part of the boundary conditions. Nevertheless, the boundary-layer equations provide a means of performing a consistency check on a turbulence closure model, the premise being that if all remaining properties of the flow are predicted by specifying $\rho_e u_e \delta^*$ (e.g., surface pressure, skin friction, and mean velocity profiles), then one can assume that the turbulence closure model is valid. Conversely, if the remaining flow properties are not predicted accurately, then the closure model must be invalid. Used in this fashion the inverse boundary-layer method is a powerful tool for evaluating turbulence closure models.

Some may question the appropriateness of applying the boundary-layer equations to flows with massive separation. However, from experience they have been found to perform much better than expected. This was demonstrated, for example, in Ref. 14 through direct comparison with solutions to the Reynolds-averaged, Navier-Stokes equations for a shock-induced separated flow. The comparisons were made by employing the results from the Navier-Stokes solutions as boundary conditions for the boundary-layer calculations. Similar pressure recoveries and mean velocity profiles were obtained for a flow with quite extensive separation (the flow case was the shock-induced, separated flow considered in this section).

The boundary-layer method of Carter solves the boundary-layer equations by relaxation. At each iteration, Eq. (11) was solved by the implicit Euler method and ν_{to} in Eq. (4) was determined by Newton's method. The number of iterations to convergence was nearly identical to that required by the Cebeci-Smith model. Interestingly, with the Cebeci-Smith model this convergence rate required the use of Newton linearization, whereas with the proposed closure model this was unnecessary.

The first test case to be presented is the axisymmetric, transonic, shock-wave/turbulent boundary-layer experiment of Bachalo and Johnson.[3] Of the three test cases considered in this paper, this one represented the severest challenge to the proposed closure model. A sketch of the flow model is presented in Fig. 1 along with the boundary-layer displacement thickness distribution that results from the strong inviscid/viscous interaction that develops on this model when $M_\infty = 0.875$. In Fig. 1b, x is the distance from the leading edge of the circular arc section and c is the chord length of the circular arc section. For the approach Mach number of 0.875, a shock wave results at $x/c \simeq 0.65$ that is sufficiently strong to produce an extensive region of separated flow. Separation occurs just downstream of the shock wave ($x/c \simeq 0.70$) and the flow does not reattach until downstream of the circular arc section ($x/c \simeq 1.15$).

The measured surface pressure distribution for this interaction and those predicted by the proposed nonequilibrium turbulence closure model (NTM) and the Cebeci-Smith model (CEBSM) are compared in Fig. 2. The NTM calculations were started using the CEBSM, with the NTM turned on well ahead of the leading edge of the circular arc section. The calculations downstream of this point were performed in the inverse mode. As is evident from Fig. 2, the NTM predicts a surface pressure distribution that is in much better agreement with experiment than that predicted by the CEBSM. The overprediction of the pressure recovery with the CEBSM is typical of this model when applied to separated flows. If a_1 had been reduced slightly, the NTM would have predicted a pressure distribution almost identical to that of the experiment. Such a fine tuning of the model at the present stage of development is probably inappropriate, however. It would be more appropriate once the model was

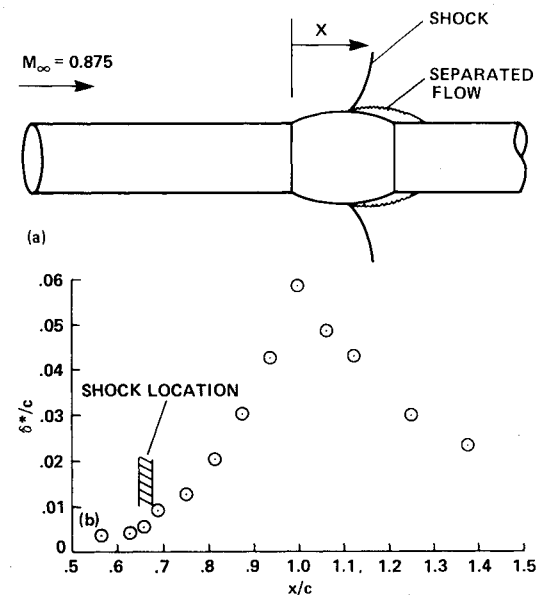

Fig. 1 Shock-induced separated flow, $M_\infty = 0.875$: a) flow model; b) boundary-layer displacement thickness distribution.

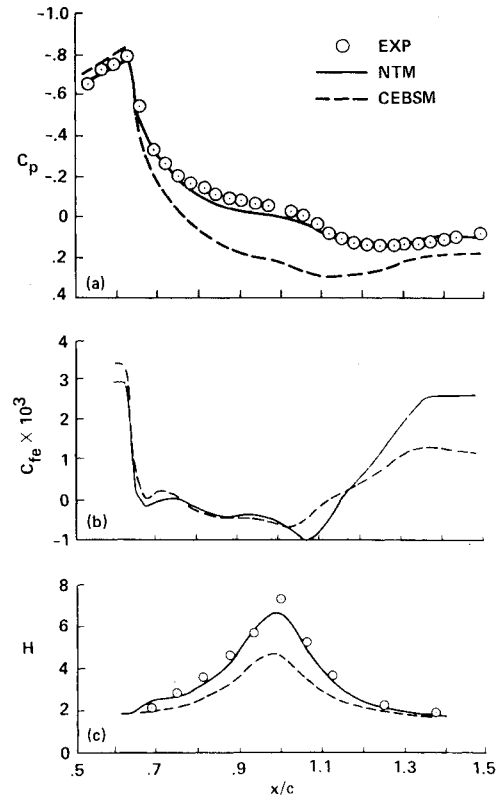

Fig. 2 Shock-induced separated flow, $M_\infty = 0.875$: a) surface-pressure distribution; b) skin-friction distribution; c) shape-factor distribution.

incorporated into a truly predictive method (i.e., a coupled inviscid/viscous calculation method or a Navier-Stokes solution method). Included in Fig. 2 are the predicted distributions for skin friction C_{fe} and shape factor H. Skin friction was not measured in the experiment, but it is important to note that the NTM predicts substantially more recovery in C_{fe} downstream of reattachment than does the CEBSM.

In Fig. 3, calculated mean velocity profiles at a few representative stations are compared with experiment. Clearly, the profiles predicted by the NTM formulation are

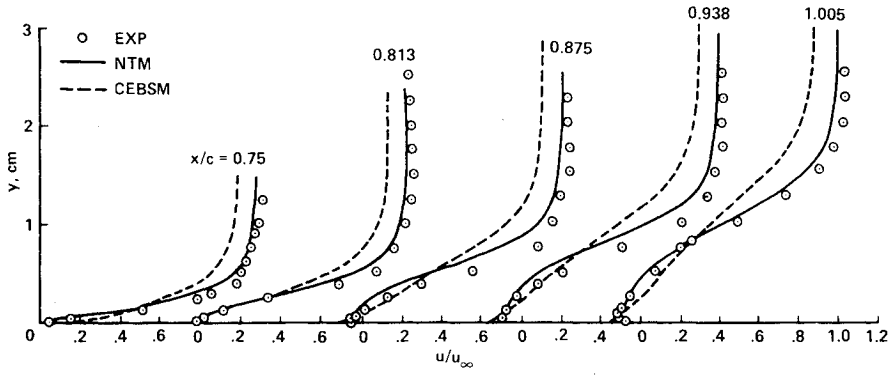

Fig. 3 Shock-induced separated flow, $M_\infty = 0.875$: mean velocity profile comparisons.

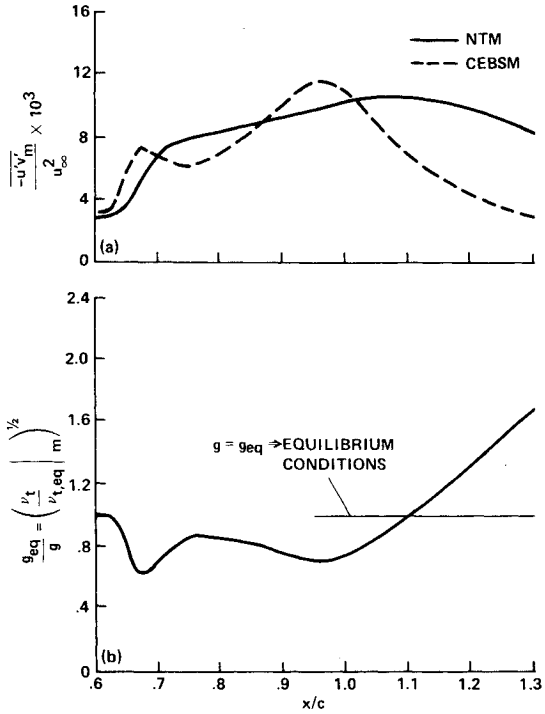

Fig. 4 Shock-induced separated flow, $M_\infty = 0.875$, "history effects": a) maximum Reynolds shear stress development; b) non-equilibrium state of flow.

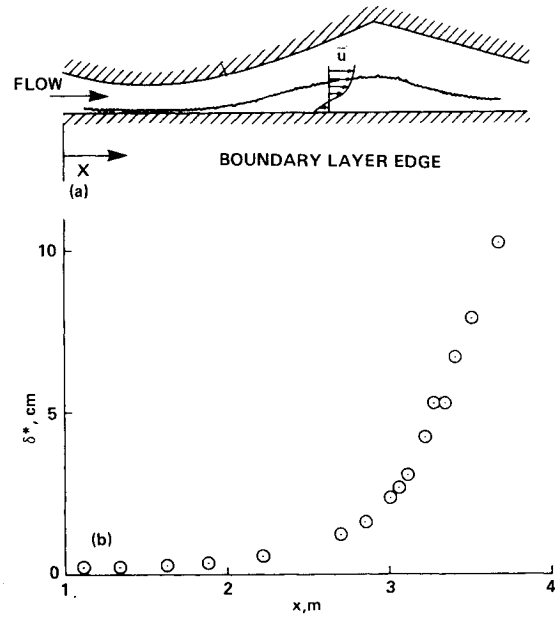

Fig. 5 Low-speed diffuser flow: a) flow model; b) boundary-layer displacement thickness distribution.

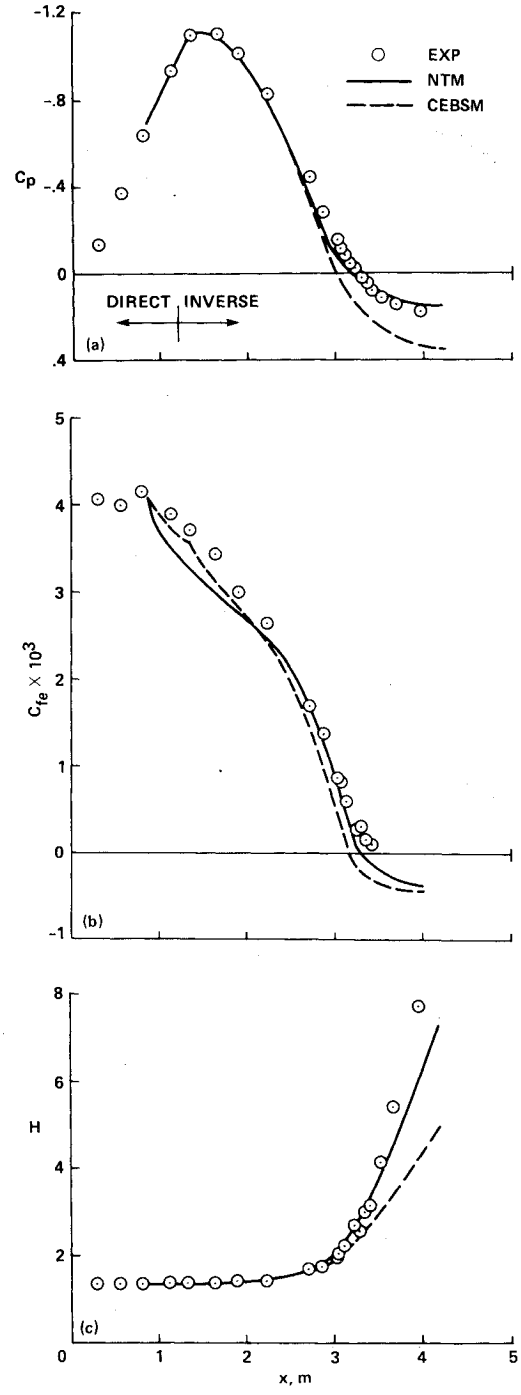

Fig. 6 Low-speed diffuser flow: a) surface pressure distribution; b) skin-friction distribution; c) shape-factor distribution.

in much better qualitative agreement with the experiment than are those predicted by the CEBSM. The smaller boundary-layer edge velocities predicted by the CEBSM are a result of the overprediction of pressure recovery. All of the profiles predicted by the CEBSM exhibit a positive curvature in the inner part of the boundary layer that is not observed in the experiment. This departure between experiment and the CEBSM results will also be seen to be present for the other flow cases considered. At $x/c-1.0$, the separated mean velocity profile predicted by the CEBSM takes on the characteristic form so often seen in the literature when this closure model is applied to separated flows. The curvature of the profile at this station is of opposite sign to that observed in the experiment and that predicted with the NTM. The misprediction in profile shape is a result of the eddy viscosity relationship used in the inner part of the boundary layer (i.e., $\nu_{ti}=D^2\kappa^2y^2\,|\partial\bar{u}/\partial y|$). It will be seen in the other flow cases to also result in mispredictions of profile shape, even well ahead of where separation occurs.

Whereas the inner eddy viscosity distribution used in the CEBSM results in poor mean velocity profile predictions, it is not the primary cause for the overprediction of pressure recovery. This is instead a result of the CEBSM predicting too rapid a rise in turbulent shear stress in the vicinity of the shock wave. On the other hand, through Eq. (11), the NTM limits the rate at which the shear stress can grow at the shock. As a result, the eddy viscosity is reduced and, therefore, the inner part of the boundary layer loses more momentum at the shock, which in turn reduces its ability to negotiate pressure gradients farther downstream. In Fig. 4, the development of $-\overline{u'v'_m}$ with streamwise distance is compared for the two closure models. Included in this figure is the quantity g_{eq}/g predicted by the NTM. This quantity, which is also equal to $(\nu_t/\nu_{t,\,eq}|_m)^{1/2}$, is a measure of the influence Eq. (11) has on the shear stress development. It also can easily be shown to equal the ratio of dissipation to production. If equilibrium were assumed, it would have the value of unity. Notice that even though the shock has the greatest influence on this quantity, even downstream of the shock, nonequilibrium effects are predicted to persist. In the recovery zone (i.e., the region where δ^* is decreasing), g_{eq}/g become greater than unity because of the slow decay in $-\overline{u'v'_m}$ predicted by Eq. (11) in this region. It is this slow decay in $-\overline{u'v'_m}$ that caused the skin friction to be higher than that predicted by the CEBSM in the region downstream of reattachment.

The next flow case to be considered is the low-speed diffuser flow studied by Simpson et al.[4] A sketch of the flow model is shown in Fig. 5. The upper surface of the diffuser is contoured to produce strong adverse pressure gradients. The lower-surface boundary layer, which undergoes massive separation because of the imposed pressure gradients, was studied in the experiment. Experimental profiles were obtained from upstream of the adverse pressure gradient region to a final downstream station where the separation became so massive that three-dimensional influences on the flow became excessive. The boundary-layer displacement thickness distribution for this experiment is included in Fig. 5.

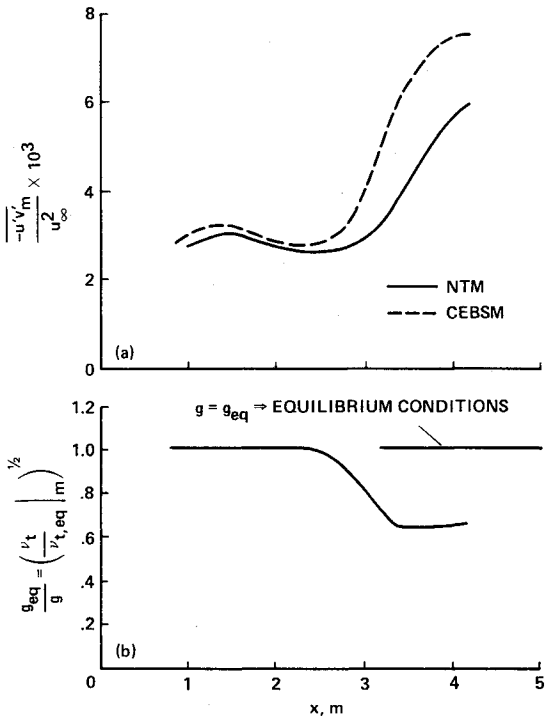

Fig. 7 Low-speed diffuser flow, "history" effects: a) maximum Reynolds shear stress development; b) nonequilibrium state of flow.

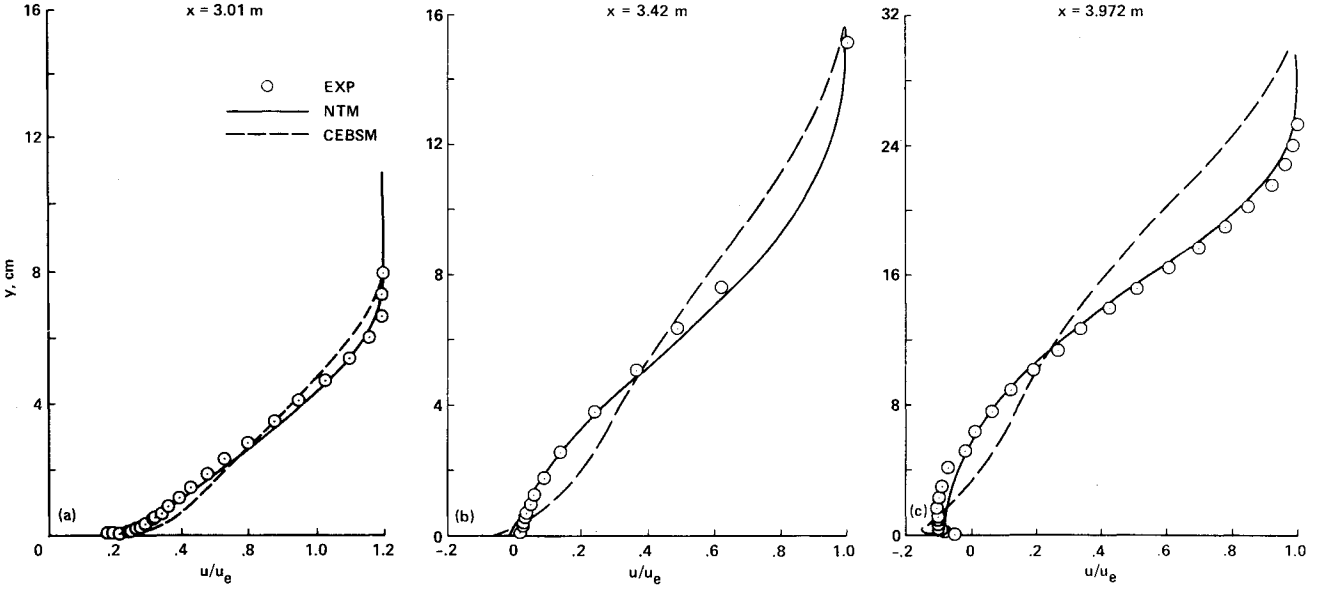

Fig. 8 Low-speed diffuser flow; mean velocity profile comparisons.

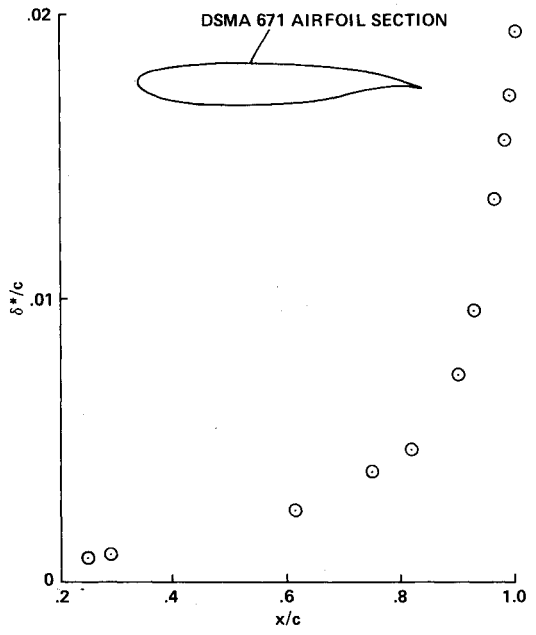

Fig. 9 Supercritical airfoil flow, $M_\infty = 0.72$ and $\alpha = 4.32$ deg: boundary-layer displacement thickness distribution.

The calculations were started from an experimentally determined mean velocity profile and a measured value for u_τ at $x = 0.8$ m. With these data available, it was not necessary to start the calculations with the CEBSM. Direct mode calculations were performed up to $x = 2.2$ m; then, from that station on, the calculations were performed in the inverse mode. Presented in Fig. 6 are the experimental and predicted surface pressure, skin-friction, and shape-factor distributions. As in the previous test case, the CEBSM predicts too large a pressure recovery, whereas the pressure recovery predicted with the NTM is in good agreement with experiment. In Fig. 7, the developments of $-\overline{u'v'_m}$ predicted by the two closure models are presented along with the quantity g_{eq}/g predicted by the NTM. These results indicate that nonequilibrium effects are also of importance for this low-speed flow. Mean velocity profiles at a few select stations are presented in Fig. 8. The trends illustrated in this figure are similar to those observed for the shock-induced separated flow. The CEBSM is seen to predict the wrong profile shape, even upstream of separation (the $x = 3.42$ station is just upstream of the measured mean separation point).

The last test case to be considered is the supercritical airfoil experiment of Johnson and Spaid.[5] This experiment was performed at conditions intended to simulate cruise. Accordingly, the shock which developed at $x/c \simeq 0.40$, on this DSMA 671 airfoil section was relatively weak, but strong aft loading resulted in a rapid growth in the boundary-layer displacement thickness along the upper surface near the trailing-edge region, as shown in Fig. 9. The boundary layer was sufficiently retarded that a small separation bubble developed at $x/c \simeq 0.98$.

The NTM calculations for this case were started with CEBSM. At $x/c = 0.22$ the NTM was turned on (a transition strip was located on the model at $x/c = 0.17$). For both closure models, the calculations were performed in the direct mode up to the shock and, from the point downstream, the calculations were performed in the inverse mode. The resultant predictions of surface pressure, shape factor, and skin friction are presented in Fig. 10. Notice that even for this flow, the CEBSM predicts that a sizable pressure gradient can be sustained even though the flow separates. This seems to be a general characteristic of CEBSM predictions. As a consequence, this model tends to overpredict airfoil performance. On the other hand, the NTM formulation predicts a pressure plateau similar to that observed experimentally when separation occurs. The results shown in Fig. 10 suggest that the NTM should do substantially better in predicting airfoil performance when it is incorporated into an airfoil prediction method. Mean velocity comparisons at representative stations are presented in Fig. 11 and the development of $-\overline{u'v'_m}$ and the quantity g_{eq}/g are presented in Fig. 12. Notice that just downstream of the shock g_{eq}/g is greater than unity. This accounts for the skin-friction values predicted in this region being larger than those predicted by the CEBSM. Also, notice how small g_{eq}/g becomes near the trailing edge, which suggests that the flow is far from equilibrium in this region.

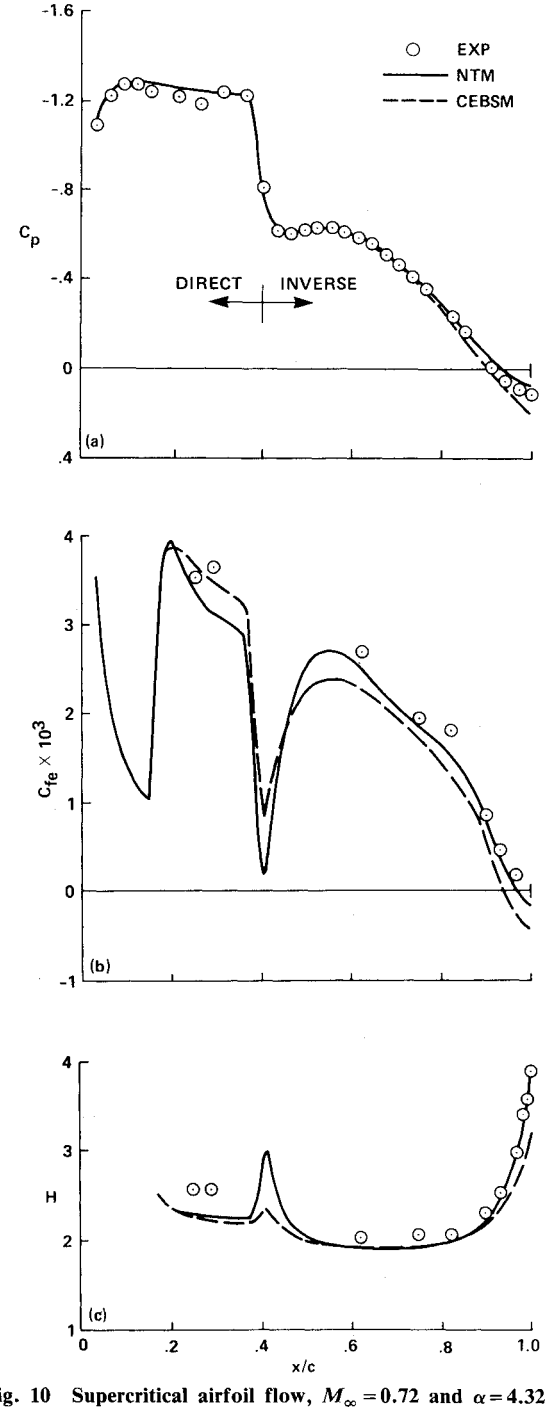

Fig. 10 Supercritical airfoil flow, $M_\infty = 0.72$ and $\alpha = 4.32$ deg: a) surface pressure distribution; b) skin friction distribution; c) shape-factor distribution.

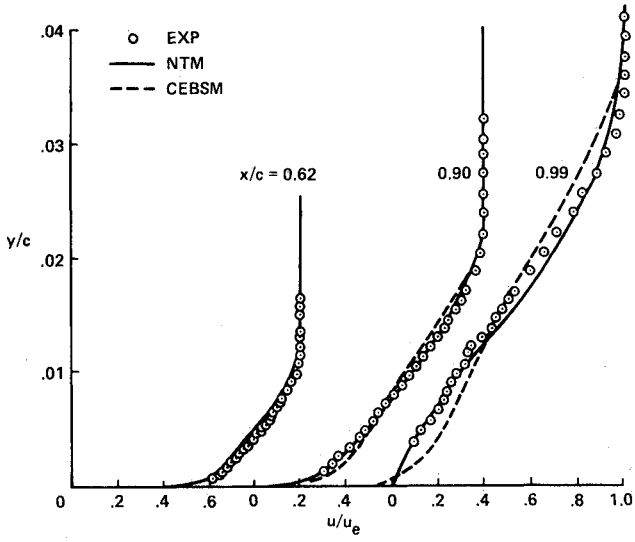

Fig. 11 Supercritcal airfoil flow, $M_\infty = 0.72$ and $\alpha = 4.32$ deg: mean velocity profile comparisons.

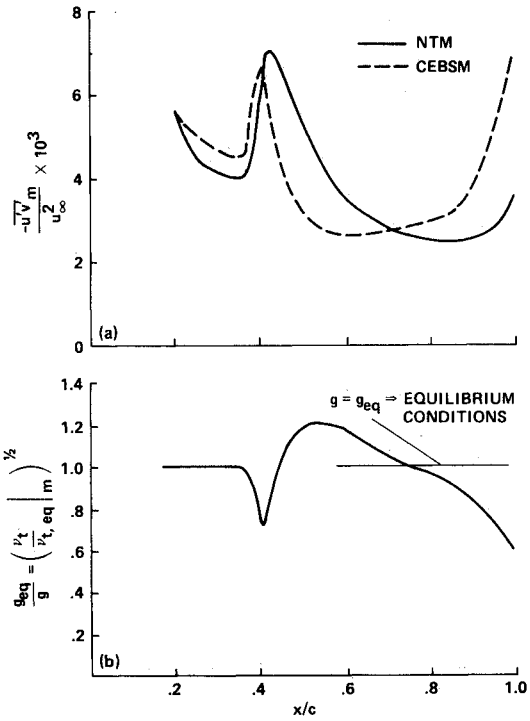

Fig. 12 Supercritical airfoil flow, $M_\infty = 0.72$ and $\alpha = 4.32$ deg "history" effects: a) maximum Reynolds shear stress development; b) nonequilibrium state of flow.

Conclusions

A new turbulence closure model has been formulated specifically for two-dimensional, turbulent boundary-layer flows subjected to severe adverse pressure gradients. Based on comparisons with experiment, this closure model appears capable of treating subsonic, pressure-driven separated flows and shock-induced separated flows. From the standpoint of engineering practicality, the proposed closure model has distinct advantages over the more complex, two-equation, eddy viscosity models. It requires only slightly more computational effort than simple closure models, such as the CEBSM, and introduces no numerical stability problems.

A report[15] is in preparation that the potential user of this closure model will likely find informative. Included in this report are aspects that for reasons of length could not be included in this paper; for example, the performance boundary layers with zero and favorable pressure gradients and the solution sensitivities to the values prescribed for the modeling constants.

The next obvious step will be to incorporate the proposed closure model into a truly predictive method. Ideally, the predictive method should be based on the Reynolds-averaged, Navier-Stokes equations, since this would eliminate the possibility of falsely attributing errors caused by approximations to the mean flow equations to the closure model. Once this is done, it will be interesting to see how the proposed model will perform against two-equation, eddy viscosity and full Reynolds stress closure models.

Appendix

In the early stages of this study, the diffusion term in Eq. (6) was assumed to be negligibly small relative to the convective term in that same equation. Calculations performed with the diffusion term neglected produced excellent results in retarded flow regions [i.e., regions where $d(-\overline{u'v'_m}/dx$ was positive and consequently, where ν_{to} was less than $\nu_{to,\,eq}$ as a result of the convective term in Eq. (6)]. However, in the downstream recovery regions the neglect of turbulent diffusion resulted in too slow a decay in $-\overline{u'v'_m}$ with the streamwise distance. Moreover, in the case where massive separation occurred upstream, the neglect of the turbulent diffusion term resulted in the outer eddy viscosities downstream becoming so large that converged solutions could not be obtained. It became obvious that turbulent diffusion could not be neglected in flow recovery regions. One solution to the problem would be to assume that the convective and diffusion terms in Eq. (6) exactly cancel each other in regions of flow recovery (i.e., that ν_{to} never exceeds $\nu_{to,\,eq}$). However, this strong assumption appears to result in too rapid a decay in $-\overline{u'v'_m}$ and also in an underprediction of skin-friction recovery.

To improve the prediction of the streamwise decay in $-\overline{u'v'_m}$ in flow recovery regions, a model for the diffusion term in Eq. (6) was formulated. The diffusion model of Bradshaw et al.[9] was not adopted since it was deemed essential that the eddy viscosity distribution reduce to the equilibrium eddy viscosity distribution of Eq. (8) in regions where the convective term in Eq. (6) was negligibly small. To accomplish this, the turbulent diffusion term as described later is related to the nonequilibrium state of flow in the outer part of the boundary layer.

Similarly to Bradshaw et al., the "bulk" convection hypothesis of Townsend[16] is used as a starting point,

$$\frac{\partial}{\partial y}\left(\frac{\overline{p'v'}}{\rho}+\frac{1}{2}\overline{q^2v'}\right)=\frac{\partial}{\partial y}(\overline{q^2}v) \tag{A1}$$

where v is a lateral convection velocity representing the turbulent transport by the larger and more energetic eddying motions. Along the path of maximum kinetic energy, Eq. (A1) takes the form:

$$\mathcal{D}_m=\frac{-\overline{u'v'_m}}{a_1}\left.\frac{\partial v}{\partial y}\right|_m \tag{A2}$$

where the relationship $-\overline{u'v'_m}/k_m = a_1$ has been assumed. An approximate model for the variation of v with y/δ as shown in Fig. A1 is proposed based on the $\overline{q^2v'}$ measurements obtained by Bradshaw[17] for two adverse pressure gradient boundary-layer flows. Based on this qualitative model, the following estimate is proposed for $\partial v/\partial y|_m$:

$$\left.\frac{\partial v}{\partial y}\right|_m \propto \frac{v_o}{\delta(0.7-y/\delta|_m)} \tag{A3}$$

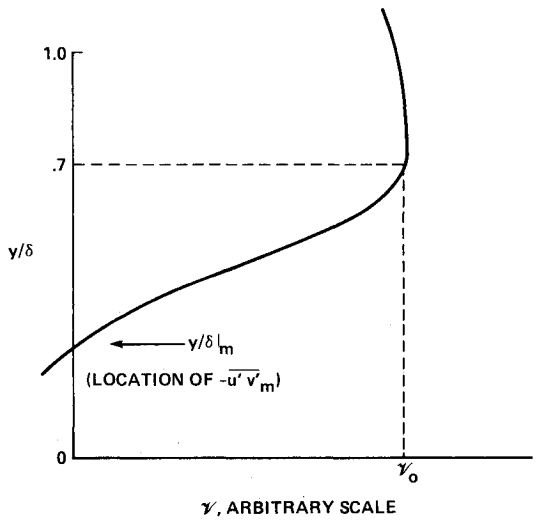

Fig. A1 Qualitative model for v as a function of y/δ.

In Eq. (A3), v_o is the maximum lateral convection velocity that is hypothesized to occur at $y/\delta \simeq 0.7$. This quantity is in turn assumed to be proportional to

$$v_o \propto (-\overline{u'v'_m})^{1/2} \left| 1 - \frac{\text{dissipation}}{\text{production}} \right|_o \quad \text{(A4)}$$

The term inside the absolute value sign represents the imbalance between production and dissipation in the outer part of the boundary layer, which can be expressed in terms of eddy viscosities,

$$\left| 1 - \frac{\text{dissipation}}{\text{production}} \right|_o = \left| 1 - \frac{(-\overline{u'v'})^{3/2}/L}{(-\overline{u'v'})\partial\bar{u}/\partial y} \right| = \left| 1 - \left(\frac{\nu_{to}}{\nu_{to,\,\text{eq}}} \right)^{1/2} \right| \quad \text{(A5)}$$

The scaling of v_o to $(-\overline{u'v'_m})^{1/2}$ in Eq. (A4) is consistent with the arguments of Townsend. The other term in Eq. (A4) has been added to make the turbulent diffusion functionally dependent on the nonequilibrium state of the flow. In regions where the flow is being retarded, the diffusion term in Eq. (6) is of the same sign as the convective term and thus can result in even larger departures from equilibrium. In regions where the flow is recovering, it opposes the convective term, hence causing a more rapid recovery to equilibrium conditions. The intent in the development of an expression for the turbulent diffusion term was to allow a more rapid return to equilibrium in flow recovery regions with a minimal change in the closure model performance in retarded flow regions. The expression given by Eq. (A4) has these properties. Combining Eqs. (A3-A5) and introducing the modeling constant, C_{dif}, Eq. (9) is obtained,

$$\mathcal{D}_m = \frac{C_{\text{dif}}(-\overline{u'v'_m})^{1/2}}{a_1\delta(0.7 - y/\delta|_m)} \left| 1 - \left(\frac{\nu_{to}}{\nu_{to,\,\text{eq}}} \right)^{1/2} \right| \quad \text{(A6)}$$

This model for the turbulent diffusion is acknowledged to be very approximate. As more experience is gained with the turbulence closure approach proposed, a more refined model for the turbulent diffusion should evolve.

Acknowledgments

The authors gratefully acknowledge the kindness of Dr. J. E. Carter of United Technologies Research Center for making available to us his boundary-layer program with documentation and his assistance during the initial stages of applying this program.

References

[1]Bradshaw, P., "The Understanding and Prediction of Turbulent Flow," *Aeronautical Journal*, Vol. 76, No. 739, 1972, pp. 403-418.

[2]Cebeci, T. and Smith, A. M. O., *Analysis for Turbulent Boundary Layers*, Academic Press, New York, 1974.

[3]Bachalo, W. D. and Johnson, D. A., "An Investigation of Transonic Turbulent Boundary Layer Separation Generated on an Axisymmetric Flow Model," AIAA Paper 79-1479, 1979.

[4]Simpson, R. L., Chew, Y. T., and Shivaprasad, B. G., "The Structure of a Separating Turbulent Boundary Layer, Part I: Mean Flow and Reynolds Stresses," *Journal of Fluid Mechanics*, Vol. 113, 1981, pp. 23-51.

[5]Johnson, D. A. and Spaid, F. W., "Supercritical Airfoil Boundary-Layer and Near-Wake Measurements," *Journal of Aircraft*, Vol. 20, April 1983, pp. 298-305.

[6]Horstmann, C. C. and Johnson, D. A., "Prediction of Transonic Separated Flows," *AIAA Journal*, Vol. 22, July 1984, pp. 1001-1003.

[7]Coakley, T. J., "Turbulence Modeling Methods for the Compressible Navier-Stokes Equations," AIAA Paper 83-1693, July 1983.

[8]Perry, A. E. and Schofield, W. H., "Mean Velocity and Shear Stress Distributions in Turbulent Boundary Layers," *Physics of Fluids*, Vol. 16, Dec. 1973, pp. 2068-2081.

[9]Bradshaw, P., Ferriss, D. H., and Atwell, N. P., "Calculations of Boundary-Layer Development Using the Turbulent Energy Equation," *Journal of Fluid Mechanics*, Vol. 28, Pt. 3, 1967, pp. 593-616.

[10]Rubesin, M. W., "Numerical Turbulence Modeling," AGARD LS-86, 1977.

[11]McDonald, H., "The Departure from Equilibrium of Turbulent Boundary Layers," *Aeronautical Quarterly*, Vol. 19, No. 1, Feb. 1968, pp. 1-19.

[12]Green, J. E., Weeks, D. J., and Brooman, J. W. F., "Prediction of Turbulent Boundary Layers and Wakes in Compressible Flow by a Lag-Entrainment Method," British Aeronautical Research Council, R&M 3791, 1977.

[13]Carter, J. E., "Viscous-Inviscid Interaction Analysis of Transonic Turbulent Separated Flow," AIAA Paper 81-1241, 1981.

[14]Johnson, D. A., Horstmann, C. C., and Bachalo, W. D., "Comparison between Experiment and Prediction for a Transonic Turbulent Separated Flow," *AIAA Journal*, Vol. 20, June 1982, pp. 737-744.

[15]Johnson, D. A. and King, L. S., "A New Turbulence Closure Approach for Two-Dimensional Boundary Layers with Separation," NASA, to be published.

[16]Townsend, A. A., *The Structure of Turbulent Shear Flow*, Cambridge University Press, Cambridge, England, 1976.

[17]Bradshaw, P., "The Turbulent Structure of Equilibrium Boundary Layers," *Journal of Fluid Mechanics*, Vol. 29, Pt. 4, 1967, pp. 625-645.